SPACE WEATHERING OF PRIMITIVE ASTEROIDS: IRON OXIDATION STATE CHANGES IN ION IRRADIATIED MURCHISON CM2 CHONDRITE MATRIX. L. P. Keller[1] and R. Christoffersen[2], [1]ARES, Code XI3, NASA/JSC, Houston, TX 77058 (Lindsay.P.Keller@nasa.gov). [2]Jacobs, NASA/JSC, Code XI, Houston, TX, 77058.

Introduction. Space weathering processes affect all airless bodies in the Solar System to some degree, and sample analyses combined with lab experiments furnish critical insights into the chemical, spectroscopic and mineralogic effects that result from exposure to the space environment. While much is known about lunar-style space weathering, the physical and chemical response of hydrated carbonaceous chondrite materials to space weathering processes is still at an early stage [1-3]. Space weathering experiments aid in the interpretation of remote-sensing data, as well as understanding regolith evolution on primitive carbonaceous asteroids. In addition, studies of this type will help guide the planning for analyses of the returned samples from the Hayabusa2 and OSIRIS-REx missions. In particular, the behavior of iron and its oxidation states play a critical role in controlling optical properties measured by remote-sensing instruments. Here, we report the results of our preliminary ion irradiation experiments on a hydrated carbonaceous chondrite with emphasis on microstructural and chemical changes, focusing on Fe oxidation state changes.

Samples and Methods. A polished thin section of the Murchison CM2 carbonaceous chondrite was irradiated with 4 kV He^+ (normal incidence) to a total dose of $1x10^{18}$ He^+/cm^2 over an area of ~5x5 mm^2 [2]. The irradiated area included abundant matrix and chondrules. We obtained *ex situ* Fourier-transform infrared (FTIR) reflectance spectra from multiple areas of matrix, ~150 μm^2 in size, using a Hyperion microscope on a Vertex Bruker FTIR bench. A JEOL 7600F field emission scanning electron microscope (SEM) was used to study the morphological effects of the irradiation. Following the SEM analyses, we extracted thin sections from both irradiated and unirradiated regions in matrix using focused ion beam (FIB) techniques. We used electron beam deposition for the protective carbon strap to minimize surface damage artifacts from the FIB milling. The FIB sections were analyzed using a JEOL 2500SE scanning and transmission electron microscope (STEM) equipped with a Gatan Tridiem imaging filter and a Thermo-Noran energy-dispersive X-ray (EDX) spectrometer. Electron energy-loss spectroscopy (EELS) data were collected from 50 nm diameter regions with an energy resolution of 0.7 eV FWHM at the zero loss peak. EELS spectra were collected uing low electron doses to minimize possible artifacts from electron-beam irradiation damage [4,5].

Results and Discussion. SEM imaging shows that the irradiated matrix regions have a "bubbly" or "frothy" texture, with numerous sub-μm rounded holes and voids relative to the un-irradiated material. TEM analysis of the FIB sections show that the frothy texture in the irradiated matrix results from the formation of irregulary-shaped 50-100 nm voids at the sample surface. In addition, there are smaller (20-50 nm dia.) vesicles in some of the surface-exposed grains.

High-resolution TEM imaging shows that the fine-grained Mg-rich serpentine group minerals have been amorphized from the He irradiation to a depth of ~150-200 nm. Assuming a target density of ~1.3 (the density of serpentine with 50% porosity), and allowing for reasonable changes in target density during the irradiation, there is excellent agreement between the total thickness of the amorphized layer and the He^+ ion damage depth obtained from SRIM calculations [6]. We obtained quantitative EDX line scans from the surface down to unirradiated matrix and did not observe any statistically significant compositional changes in Mg, Si, S, and Fe. Large (μm-sized) FeNi sulfides exposed at the surface however, show a preferential loss of sulfur by sputtering and the development of a thin 5-10 nm rim of nanophase Fe metal, similar to experimentally irradiated FeS [7]. A sub-μm $CaCO_3$ grain also appears to have been amorphized by the He^+ irradiation.

There is a distinct chemical shift in the Fe $L_{2,3}$ edge position for EELS spectra from Fe^{2+} versus Fe^{3+} phases (Figure 1). The Fe $L_{2,3}$ EELS spectra we obtained from the the Mg-rich phyllosilicates in Murchison matrix show mixed Fe^{2+}/Fe^{3+} oxidation states. The Fe $L_{2,3}$ spectra from the irradiated/amorphized matrix phyllosilicates show higher Fe^{2+}/Fe^{3+} ratios compared to spectra obtained from pristine material at depths beyond the implantation/amorphization layer. We used well-characterized standards to fit the L_3 edges to obtain qunatiative Fe^{2+}/Fe^{3+} ratios. The unirradiated Mg-rich phyllosilicates have a ratio of Fe^{2+}/Fe^{3+}=0.28, wheras the irradiated phyllosilicates show an enhanced ratio of Fe^{2+}/Fe^{3+} =0.52 (Figures 2 and 3). We found no evidence from the EELS data for the presence of metallic Fe in the irradiated material. We also obtained O *K* spectra from phyllosilicates in both regions of the sample. The O *K* spectra show a pre-edge feature at ~530.5 eV that is related to O 2*p* states hybridized with Fe 3*d* states [5]. The intensity ratio of the O *K* pre-edge peak relative to the main part of the O *K*

edge (that results from transitions of O 1*s* to 2*p* states) is lower in the irradiated layer compared to the pristine material and may reflect the loss of O (as OH) as was observed by IR spectroscopy [2].

Conclusions. Irradiation of Murchison matrix with 4 keV He^+ produced several results including: the amorphization of the phyllosilicates to a depth of ~200 nm, blistering and void development, and a loss of OH from the hydrated silicates. In addition to these effects, EELS spectra of He^+ irradiated matrix serpentines show that they are significantly reduced during irradiation with an ~ 2X increase in Fe^{2+}/Fe^{3+} in the irradiated material compared to the un-irradiated serpentine.

References. [1] Lantz, C. *et al.* (2015) A&A, 577, A41. [2] Keller, L. P. et al. (2015) LPSC 44th, #1913. [3] Laczniak, D. L. et al. (2019) MAPS, #6434. [4] Garvie, L. A. *et al.* (2004) *Am. Min.* 89, 1610. [5] Garvie, L. A. (2010) *Am. Min.* 95, 92. [6] Ziegler, J.F. *et al.* (2006) Stopping and Range of Ions in Matter http://srim.org. [7] Keller, L. P. *et al.* (2013) *LPSC XLIV*, #2404.

Acknowledgements. This work was supported by grants from the NASA R&A Programs. We thank the USNM for the Murchison chip used in this study.

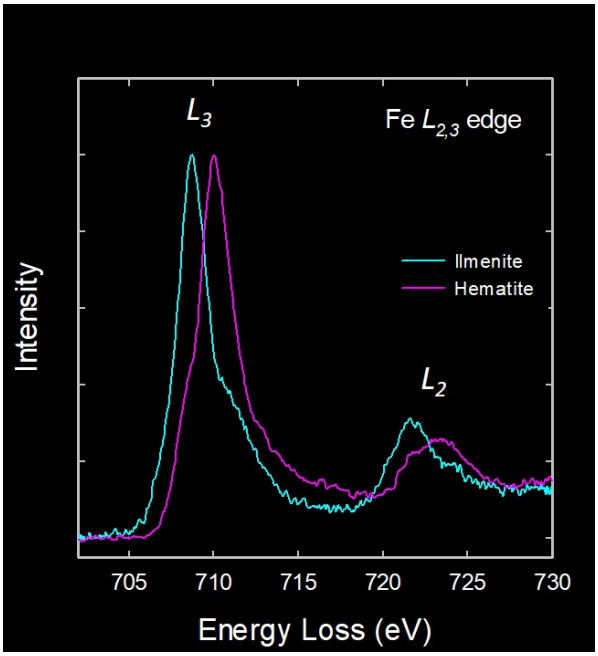

Figure 1. EELS spectra showing the chemical shift in the position of the $L_{2,3}$ peaks between Fe^{2+} and Fe^{3+}.

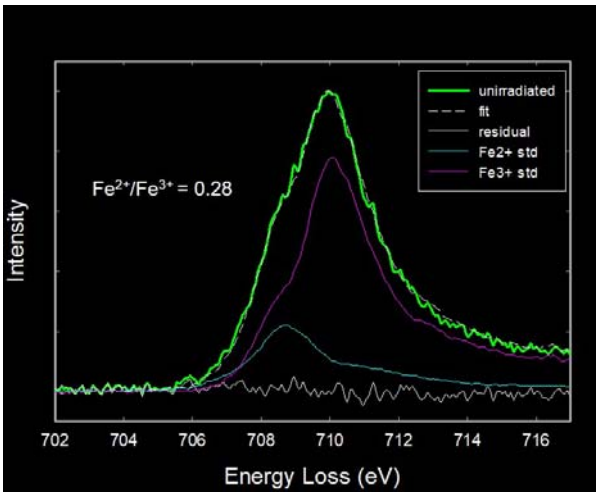

Figure 2. Fitting of the Fe L_3 edge in unirradiated Mg-rich serpentine in Murchison matrix showing Fe^{2+}/Fe^{3+}=0.28 and the resulting fit and residual.

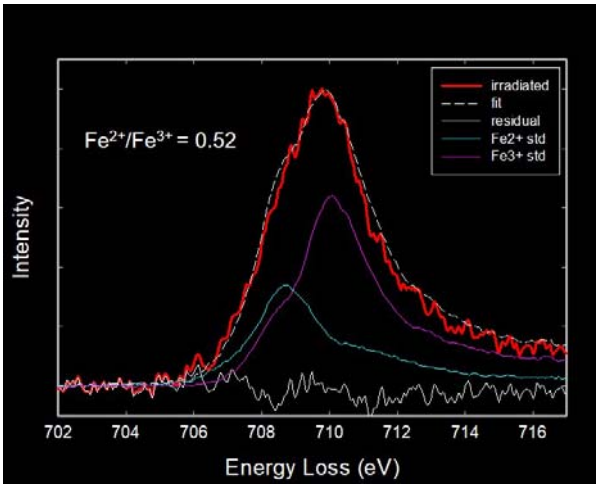

Figure 3. Fitting of the Fe L_3 edge in irradiated Mg-rich serpentine in Murchison matrix showing Fe^{2+}/Fe^{3+}=0.52 and the resulting fit and residual.